Supporting Information

High throughput and selective enrichment of histidine-tagged enzymes with Ni-doped magnetic mesoporous silica

Jiho Lee,[†,‡] Soo Yeoun Lee,[†] So Hyun Park,[†] Hye Sun Lee,[†] Jinhyung Lee,[†] Bong Yong Jeong,[†] Sang Eon Park,[‡] and Jeong Ho Chang*[,†]

[†]Bio-IT Convergence Center, Korea Institute of Ceramic Engineering and Technology, Seoul 153-801, Korea, and [‡]Department of Chemistry, Inha University, Incheon 402-751, Korea

Confirmation of Fe nanoparticles within the mesoporoes by cross-section high resolution TEM

The cross-sectional specimens were analyzed by JEM-2000EX TEM (JEOL, Japan) microscope operated at 400 kV. For the cross-sectional TEM studies, the multilayer sample was sandwiched between two Si plates and thinned by ion bombardment until perforation.

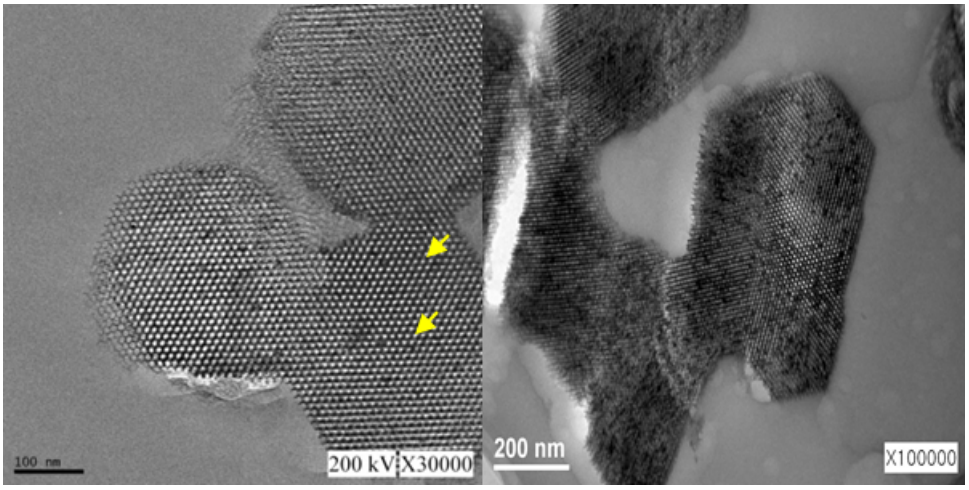

Figure S1. Low magnification and high magnification cross-section HR-TEM images of Fe nanoparticles within the mesopores.

BET isotherms of Fe-MMS as a function of thermal hydrogenation

The BET surface areas of the synthetic materials are determined by the nitrogen adsorption-desorption method to confirm the change in the porosity of Fe containing magnetic mesoporous silica (MMS) as a function of hydrogen reduction temperature. Fe-MMS materials show the shift in hysteresis position to higher relative pressure and a decreasing trend as a function of thermal hydrogenation reduction. The shift of the sharp inflection in the P/P_0 is changed to higher relative pressure of 0.75, 0.83, and 0.9 corresponding to Fe-MMS_{400}, Fe-MMS_{500}, and Fe-MMS_{600} from 0.64 of MS. This result implies the change of porosity as a function of thermal hydrogenation from mesoporous to macroporous structure through the multi-modal porosity as shown in BJH plot.

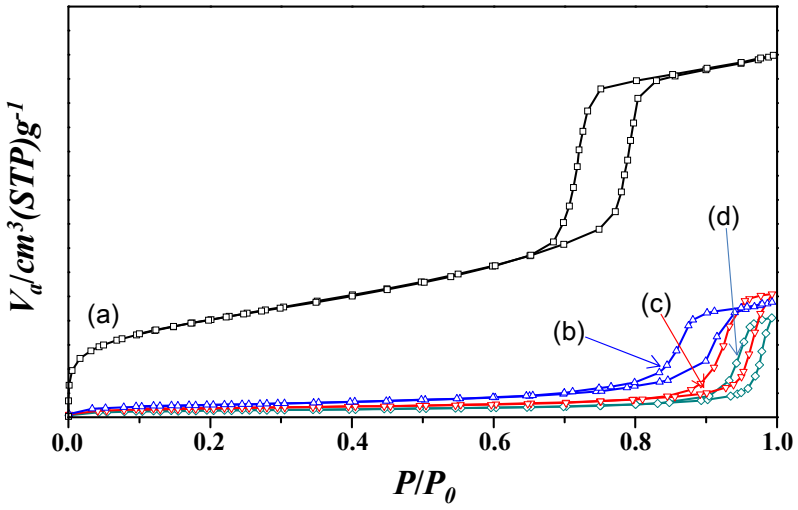

Figure S2. BET isotherms and pore-size distribution by BJH plot of Fe-MMS as a function of thermal hydrogenation. ((a) MS, (b) Fe-MMS_{400}, (c) Fe-MMS_{500}, and (d) Fe-MMS_{600}).

Quantitative analysis for Fe and Ni species in Fe-MMS and Ni-MMS by ICP-OES

For a quantitative analysis of the iron oxide species formed in mesopores at various hydrogen reduction temperatures, inductively coupled plasma optical emission spectrometry (ICP-OES) measurements were carried out through titration. The Fe^{2+} and total Fe content in the mesopores were determined as functions of the hydrogen reduction temperature by ICP-OES. The titration method employed was a modified version of a method reported in the literature.

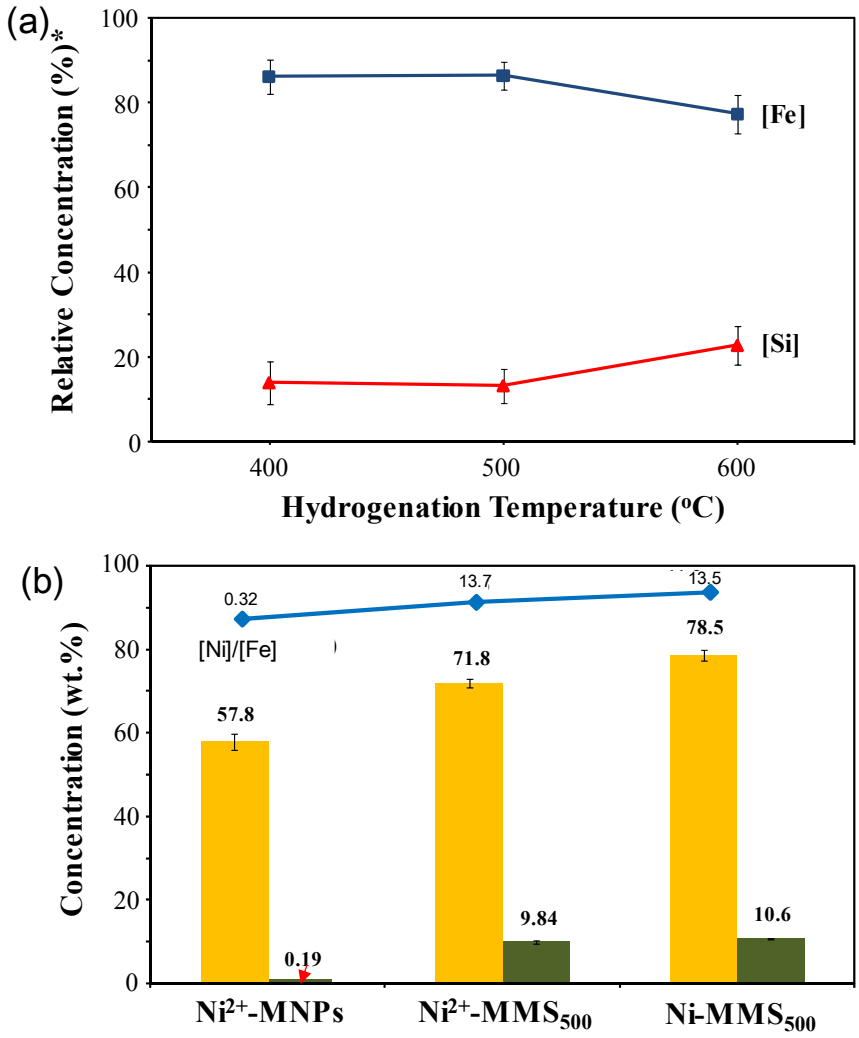

Figure S3. ICP-OES analysis of the Fe-MMS and Ni-MMS. (a) [Fe] and [Si] concentration of the Fe-MMS as functions of thermal hydrogenation reduction. (* Relative concentration means ([Fe] or [Si])/ ([Fe]+[Si]). (b) [Fe] and [Ni] concentration of the Ni-MMS and the Ni-MNPs. ([Ni]/[Fe] ratio of the sample is inserted).

Heterologous expression of histidine-tagged CatA enzyme

The *catA* coding region was amplified from the chromosomal DNA of *C. glutamicum* ATCC 13032 by polymerase chain reaction (PCR) using the primer pair. The PCR product was digested with *Nde*I/*Not*I and ligated into the *Nde*I/*Not*I-restricted plasmid, pET-21a. The resulting plasmid pSY-Cat was transferred to *E. coli* BL21 (DE3) by electroporation. The synthesis of the six histidine-tagged CatA fusion protein was induced in recombinant *E. coli* BL21 (pSY-Cat) by the addition of 0.5 mM IPTG after the culture had reached an optical density at 600 nm of 0.6. The cells were grown for 3 h. Purification of the fusion protein was carried out by affinity chromatography (Ab Frontier Inc., Korea). 1 mg Ni-MNPs were added to purified CatA solution in 10 mM phosphate buffered saline (PBS, pH 7.4) and incubate with shaking for 1 h. CatA conjugated Ni-MMS (CatA@Ni-MMS) were separated from the solution using a magnet for 1 min, and washed with PBS briefly. Proteins were analyzed by SDS-PAGE and their concentrations estimated by standard bicinchoninic acid protein assay using Pierce BCA Protein Assay kit (Thermo Scientific Inc., USA).

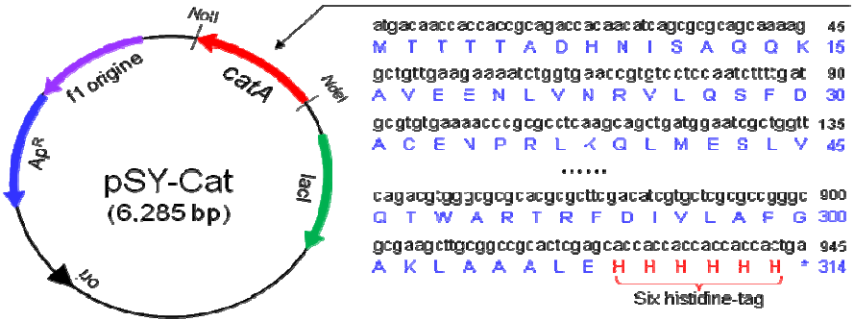

Figure S4. Plasmid construction for six histidine-tagged catechol 1,2-dioxygenase (CatA-His_6) synthesis.

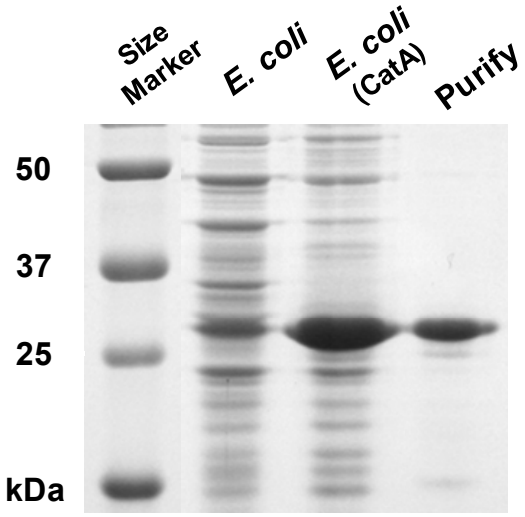

Figure S5. Agarose gel electrophoresis image of synthesis of six histidine-tagged CatA from *E.coli*.

Spherical core/shell-type Ni^{2+}-functionalized silica-coated magnetic nanoparticles (Ni^{2+}-MNPs)

Fe_3O_4 magnetite was prepared by co-precipitation with Fe^{2+} and Fe^{3+}. To prepare the Fe_3O_4 magnetite, a fresh mixture of 2 M $FeCl_2 \cdot 4H_2O$ and 1 M $FeCl_3 \cdot 6H_2O$ was added to 0.7 M ammonia solution with vigorous stirring. The obtained Fe_3O_4 magnetite was separated by magnet and the supernatant was decanted. The collected Fe_3O_4 magnetite was washed 4 times with ethanol and then air-dried. Before the silica-coating process, the 100 mg Fe_3O_4 magnetite was dispersed in 100 mL cyclohexane under sonication for 3h in the presence of 3.3 mL oleic acid. The 44 g Igepal CO-520 dissolved solution in 900 mM cyclohexane was added to Fe_3O_4 magnetite solution and then further stirred for 15 min. Then, 8mL of aqueous ammonia solution was added drop wisely into the freshly prepared solution with stirring for 15 min. After stirring, a solution of 98 % tetraethyl ortho-silicate (TEOS) was added drop-wise. The mixed solution was further stirred for 20 h. Methanol was added to the solution to form dark precipitates, which were collected through centrifugation after removal of supernatants. The dark precipitate was washed repeatedly with ethanol and then vacuum dried. For Ni-MNPs preparation, 1M nickel (II) chloride hexahydrate ($NiCl_2 \cdot 6H_2O$) and MNPs were reacted in deionized water through shacking at room temperature for 1h. The final product was collected and washed with deionized water three times and then air-dried. Figure S7 shows TEM image of Ni-MNPs with 40 nm diameter (average size).

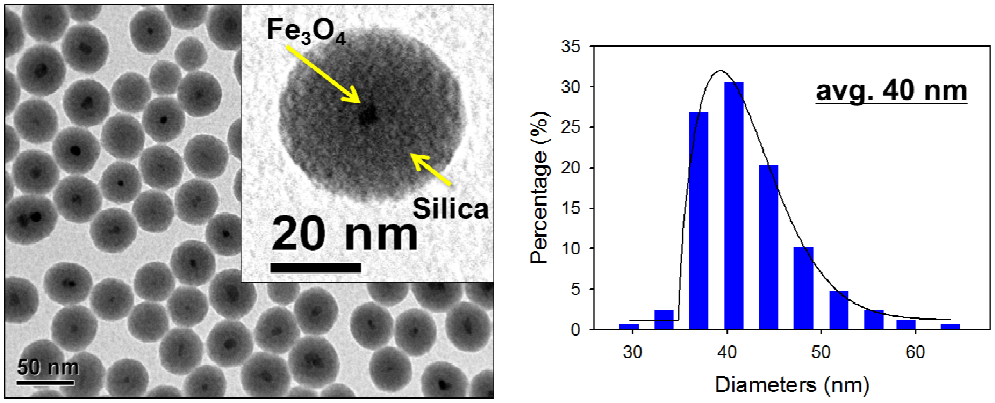

Figure S6. TEM image of Ni^{2+}-MNPs and pore-size distribution.

Table S1. Surface area and pore volume of Ni^{2+}-MMS, Ni-MMS and Ni^{2+}-MNPs

Materials	Surface area (m^2/g)	Pore volume (cm^3/g)	Source
Ni^{2+}-MMS_{500}	67	0.382	This work
Ni-MMS_{500}	110	0.313	This work
Ni^{2+}-MNPs	50	0.11	[Ref 25]*

* Lee. S.; Lee, S.; Kho, I. H.; Lee, J. H.; Kim, J. H.; Chang, J. H. *Chem. Commun.* **2011**, 47, 9989-9991.